Structural and functional characterization of the human NBC3 sodium/bicarbonate co-transporter carboxyl-terminal cytoplasmic domain

Frederick B. Loiselle, Paul Jaschke and Joseph R. Casey*

CIHR Membrane Protein Research Group, Department of Physiology and Department of Biochemistry, University of Alberta, Edmonton, Alberta, Canada T6G 2H7

Summary

The sodium bicarbonate co-transporter, NBC3, is expressed in a range of tissues including heart, skeletal muscle and kidney, where it modulates intracellular pH and bicarbonate levels. NBC3 has a three-domain structure: 67 kDa N-terminal cytoplasmic domain, 57 kDa membrane domain and an 11 kDa C-terminal cytoplasmic domain (NBC3Ct). The role of C-terminal domains as important regulatory regions is an emerging theme in bicarbonate transporter physiology. This study determined the functional role of human NBC3Ct and characterized its structure using biochemical techniques. The NBC3 C-terminal domain deletion mutant (NBC3ΔCt) had only $12 \pm 5\%$ of wild-type transport activity. This low activity is attributable to low steady-state levels of NBC3ΔCt and almost complete retention inside the cell, as assessed by immunoblots and confocal microscopy, suggesting a role of NBC3Ct in cell surface processing. To characterize the structure of NBC3Ct, amino acids 1127–1214 of NBC3 were expressed as a GST fusion protein (GST.NBC3Ct). GST.NBC3Ct was cleaved with PreScission Protease™ and native NBC3Ct could be purified to 94% homogeneity. Gel permeation chromatography and sedimentation velocity ultracentrifugation of NBC3Ct indicated a Stokes radius of 26 and 30 Å, respectively. Shape modelling revealed NBC3Ct as a prolate shape with long and short axes of 19 and 2 nm, respectively. The circular dichroism spectra of NBC3Ct did not change over the pH 6.2–7.8 range, which rules out a large change of secondary structure as a component of pH sensor function. Proteolysis with trypsin and chymotrypsin identified two proteolytically sensitive regions, R1129 and K1183-K1186, which could form protein interaction sites.

Keywords: Sodium/bicarbonate co-transport, NBC3, C-terminal tail, pH regulation, partial proteolysis.

Introduction

Regulation of intracellular pH (pH_i) is critically important in all cells as intracellular pH influences membrane transport, cell volume, metabolism and intracellular messengers (Lubman and Crandall 1992, Boron et al. 1997, Komukai et al. 1998). Physiological changes in metabolic proton production and ambient CO_2 make it necessary for cells to have a robust system to maintain pH_i homeostasis. Most cells experience transient alkalosis and acidosis, so that mechanisms for acid influx and efflux are required. Transport processes that regulate pH_i include Na^+/H^+-exchange, Na^+-dependent and -independent Cl^-/HCO_3^- exchange (AE) and monocarboxylate/H^+ and Na^+/HCO_3^- co-transport (NBC) (Igarashi et al. 1991, Juel 1996, Amlal et al. 1999, Avkiran and Haworth 1999, Chow 1999, Leviel et al. 1999, Hara et al. 2000, Hume et al. 2000). AE, Na^+-dependent AE and NBC are part of a super-family of HCO_3^- transporters (BT) (Alper et al. 2001, Sterling and Casey 2002). NBC participates in both alkalinization and acidification pathways (Gross et al. 2001). For example, in kidney tubule epithelium, NBC activity is involved in HCO_3^- reabsorption (acid secretion), while in pancreatic duct cells, NBC activity facilitates HCO_3^- secretion into the lumen of the pancreatic duct.

NBC activity has been characterized in several tissues including kidney, pancreas, conjunctiva, heart, skeletal muscle and respiratory epithelia (Abuladze et al. 1998, Pushkin et al. 1999a, Turner et al. 2001). The recent cloning of three isoforms of NBC, — NBC1, NBC3 and NBC4, — each with several splicing variants, has enabled the study of NBC activity at the molecular level (Romero et al. 1997, Abuladze et al. 1998, Burnham et al. 1998, Romero et al. 1998, Choi et al. 1999, 2000, Pushkin et al. 1999a, 2000a,b, Thevenod et al. 1999, Bevensee et al. 2000, Wang et al. 2001). NBC1 exhibits electrogenic, 3:1 or 2:1 HCO_3^- : Na^+ co-transport in the kidney and pancreas, respectively (Gross et al. 2001). NBC3 functions with an electroneutral mechanism with a 1:1 stoichiometry (Pushkin et al. 1999a). NBC4 transport is either electroneutral or electrogenic, depending on the spicing variant (Sassani et al. 2002). All three isoforms share a three-domain structure with a large N-terminal cytoplasmic domain, a highly conserved membrane domain of ~ 57 kDa, with 12 putative membrane spanning segments, and a small C-terminal domain of ~ 10 kDa. The N-terminal cytoplasmic domain of NBC3 is considerably larger than the other family members with a predicted molecular weight of 133 kDa, due in large part to an ~ 120 amino acid insert of unknown function that is absent from the other family members.

In the kidney, NBC3 is expressed in the connecting tubule and the cortical and medullary collecting duct in both type A and B intercalated cells (Pushkin et al. 1999b, Kwon et al. 2000). Interestingly, membrane targeting is cell type specific with apical or basolateral localization in type A or B cells, respectively (Kwon et al. 2000). At the sub-cellular level, NBC3 co-localizes with the vacuolar H^+-ATPase to perimembranous vesicular structures inside the plasma membrane (Pushkin et al. 1999b). This arrangement suggests that NBC3 undergoes regulated recruitment to the plasma membrane. These characteristics of NBC3 are likely mediated by interactions of its cytoplasmic domains with cytoskeletal scaffolding and targeting factors. The C-terminal domain of NBC1 (NBC1Ct) has recently been implicated in the regulation of NBC1 transport function. NBC1Ct binds carbonic anhydrase (CA) II and this binding is essential for full transport activity (Alvarez, Loiselle and Casey, submitted

*To whom correspondence should be addressed.
e-mail: joe.casey@ualberta.ca

for publication). In addition, CAII binding shifts the transport stoichiometry from 1:2 to 1:3 Na^+:HCO_3^-, and likely accounts for the tissue-type specific stoichiometry of this transporter (Gross *et al.* 2002). The NBC3 C-terminal domain also contains the consensus binding motif for CAII and the possibility of a functional interaction is currently under investigation.

The NBC3 C-terminal domain has also been implicated in regulation of transport activity through other protein/protein interactions. Recently, NBC3 was found to associate with the cystic fibrosis gene product, the Cl^- channel, CFTR, in interactions dependent on the C-terminal PDZ site on NBC3 (Park *et al.* 2002).

The objectives of this study were to determine the functional importance of the C-terminal cytoplasmic domain of human NBC3 (NBC3Ct) and to characterize its structure using biochemical techniques. Specifically, the functional role of NBC3Ct was characterized by measuring the rate of pH recovery from acid loads in cells expressing NBC3 variants. The effect of deletion of NBC3Ct on surface processing of NBC3 was examined by confocal microscopy and immunoblotting. The structure of recombinant over expressed NBC3Ct was assessed by gel permeation chromatography (GPC), velocity ultracentrifugation, circular dichroism spectroscopy (CD) and limited proteolysis. The data presented here provides a picture of NBC3Ct shape, secondary structure and identifies surface-exposed regions. This work also sets the stage for obtaining a crystal structure and allows for an independent verification of that structure.

Results

Effect of NBC3 C-terminal deletion on HCO_3^- transport

Cl^-/HCO_3^- exchangers of the AE family share up to 40% amino acid identity with NBC isoforms (Romero *et al.* 1998). Alignment of the NBC3 amino acid sequence with AE1, whose C-terminal domain has been structurally characterized (Lieberman and Reithmeier 1988; Zhu *et al.* 2003), indicates that the C-terminal tail of NBC3 spans T1127 to L1214 (not shown). To examine the functional role of the NBC3 C-terminal tail, the haemaglutinin (HA) tagged mutant HANBC3ΔCt with T1127-L1214 deleted was prepared. Transfected HEK293 cells were loaded with the pH sensitive dye, 2′,7′-bis-(2-carboxyethyl)-5-(and-6)-carboxyfluorescein-acetoxymethyl ester, subjected to acid loading and their rate of pH_i recovery was assessed (Figure 1(a)). All experiments were performed in the presence of 10 μM 5-(N-Ethyl-N-isopropyl)amiloride to inhibit endogenous Na^+/H^+-exchange activity of the HEK293 cells. HANBC3 transport activity was 2.2 ± 0.3 mM HCO_3^-/min, which is about 2-fold over background (Figure 1(a)). The transport rate of HANBC3ΔCt was determined by normalizing HANBC3 transport to 100% for each day of experiments. HANBC3ΔCt transport rate was $12\% \pm 5\%$ of HANBC3 ($n = 9$, $p < 0.05$ (unpaired, 2 tailed *t*-test)) (Figure 1(b)), indicating that loss of NBC3Ct greatly reduced transport activity. Comparison of the rate of pH_i recovery is shown in Figure 1(c). The minimum pH of cells transfected with HANBC3 and

HANBC3ΔCt cDNAs was the same (pH 6.5). However, the empty vector control acidified to pH 6.7 and, thus, recovery was less affected by intracellular buffer capacity, β_i, which accounts for the sub-background recovery of the deletion construct in this example.

NBC3 expression and localization in HEK293 cells

The diminished HCO_3^- transport activity of HANBC3ΔCt could result from reduced expression or processing of the protein to the cell surface or an effect on transport catalysis. The expression and localization of wild type NBC3 and NBC3ΔCt were assessed by immunoblotting and confocal microscopy. Immunoblots were also prepared in parallel with transport assays for each day of experiments to ensure consistent expression levels. Figure 2(a), shows an immunoblot of lysates prepared from the same transfection used to generate the transport data shown in Figure 1(c). HANBC3 migrated as two bands: a strong band at 168 kDa and a weaker band at 156 kDa. HANBC3ΔCt expression level was much lower than HANBC3 and migrated as a single weaker band at 146 kDa. The two band pattern of HANBC3 suggests that some of the protein is retained intracellularly, either unglycosylated or only core glycosylated. Since deletion of the C-terminal domain of NBC3 removes ∼10 kDa, the single HANBC3ΔCt band migrating at 10 kDa less than the lower NBC3 band suggests that the deletion is not glycosylated and may be largely retained within the cell. The dramatically lower expression level of HANBC3ΔCt may be attributable to degradation of destabilized, intracellular-retained protein, which suggests that NBC3Ct plays a role in targeting and/or folding of the transporter.

Confocal immunofluorescence microscopy of transiently transfected HEK293 cells showed that HANBC3ΔCt is largely contained within the cell (Figure 2(c)). HANBC3 also appears to be slightly intracellular-retained; however, the majority of the protein localizes to the plasma membrane (Figure 2(b)), which is consistent with a previous report that indicates that NBC3 localizes both to the plasma membrane and to a peri-plasma membrane sub-cellular pool in type A intercalated cells (Pushkin *et al.* 1999b). Taken together, the expression data and confocal microscopy suggest that deletion of the NBC3 C-terminal domain blocks the ability of the protein to reach the plasma membrane, leading to protein degradation and reduced steady-state accumulation. However, since the transport activity of HANBC3ΔCt is slightly above background, HANBC3ΔCt molecules processed to the cell surface retain some transport activity.

Over-expression and purification of NBC3Ct

Since NBC3Ct is required for NBC3 plasma membrane localization and transport activity, one chose to characterize the domain's properties. Codons 1127−1214 of human NBC3 cDNA, encoding NBC3Ct, were sub-cloned in frame, with an N-terminal GST fusion partner into the pGEX-6p-1 prokaryotic expression vector. In this construct, a PreScission protease consensus cleavage linker-sequence separates GST from NBC3Ct. GST.NBC3Ct was expressed to ∼20% of total protein in *E. coli* (Table 1, Figure 3(a)).
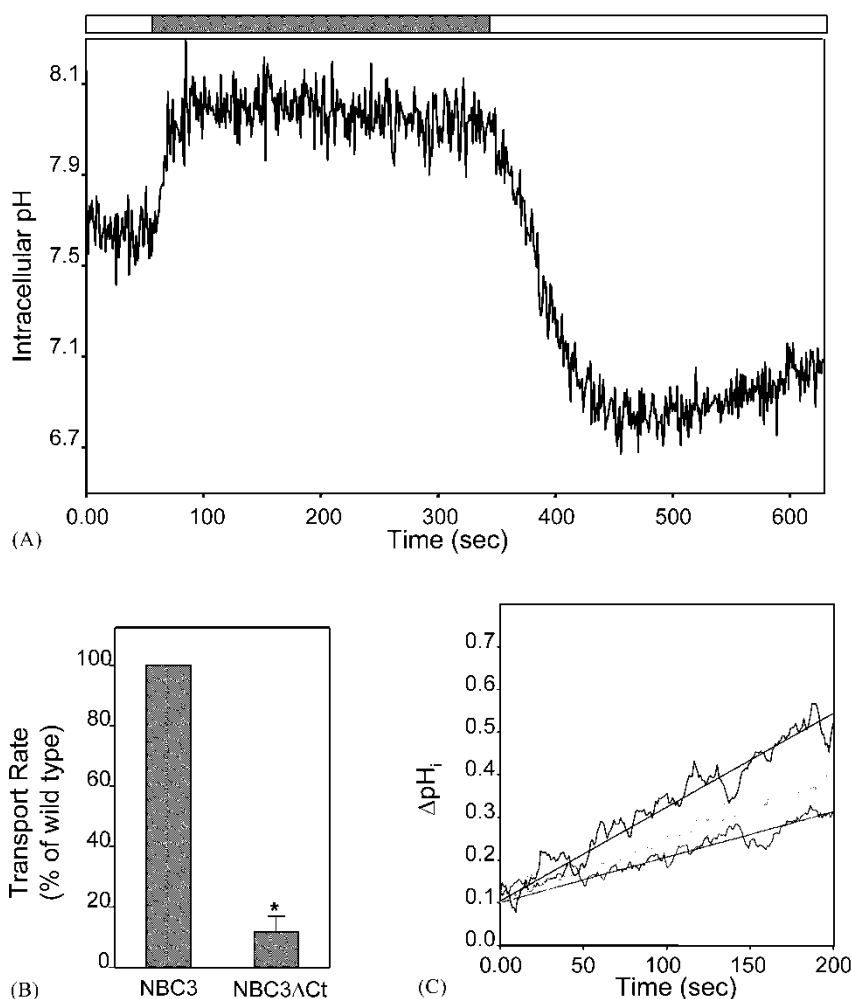
Figure 1. Functional role of NBC3Ct. (*a*) HEK293 cells grown on coverslips were transiently transfected with empty vector, HANBC3 or HANBC3ΔCt cDNAs. Transfected cells were loaded with 2′,7′-bis-(2-carboxyethyl)-5-(and-6)-carboxyfluorescein-acetoxymethyl ester and placed into a cuvette to monitor pH_i. Cells were perfused alternately with Ringers buffer (diagonal-striped bar) or Ringers buffer, containing 40 mM NH_4Cl (vertical-striped bar). Representative plot of pH vs time for cells transfected with HANBC3, where pH_i recovery rate was 0.045 ΔpH/min or 3.0 mM HCO_3^-/min. (*b*) The average pH_i recovery rate of HANBC3ΔCt is expressed as a percentage of the wild-type rate. Error bars represent standard error of the mean ($n = 9$). Asterisk represents statistical difference $p < 0.05$ (unpaired, 2 tailed *t*-test). (*c*) Representative pH_i recovery of empty vector, HANBC3 and HANBC3ΔCt transfected cells.

GST.NBC3Ct was almost completely soluble as seen by the small difference in purity between the resuspended culture and the cleared lysate (Table 1, Figure 3(*a*)). During purification, the GST-Sepharose was completely saturated with GST-NBC3Ct (∼ 8 mg GST/ml resin), so that most of the fusion protein was lost during the wash steps, which accounts for the large decrease in yield. Following cleavage with PreScission protease, the apparent purity of the preparation dropped somewhat, which was expected as ∼ 2/3 of the molecular weight of the fusion protein was lost following removal of the GST moiety; in addition, the presence of a band at ∼ 46 kDa suggests that some of the PreScission protease (which contain a GST domain) did not remain bound to the resin (Table 1, Figure 3(*a*)). A final step of GPC effectively purified NBC3Ct (Figure 3(*a*)). Two major peaks (pools A and B) were observed during GPC (Figure 4(*a*)). SDS-PAGE revealed three major bands in pool

A, likely corresponding to GST, a bacterial protein product of the *E. coli* gene dnaK known to bind GST (Sherman and Goldberg 1992), and PreScission protease (not shown). SDS−PAGE of pool B indicated a strong band with a molecular weight of 14 kDa and a much weaker slightly lower band, likely a truncated version of NBC3Ct (Figure 3(*a*)). Immunoblotting of the pools with an anti-NBC3 antibody indicated that the band from pool B corresponds to NBC3Ct (not shown). Scanning and densitometry of Coomassie blue-stained SDS-PAGE gels showed that pool A protein was 94% pure NBC3Ct (Table 1, Figure 3(*a*)). Purity was also assessed by mass spectrometry and reverse phase high performance liquid chromatography (Figure 3(*b*) and (*c*)). Mass spectrometry showed that the major peak had mass 11 165.6 Da, consistent with NBC3Ct. The small peak with m/z 22329.0 is consistent with dimeric NBC3Ct and likely represents a mass spectrometry artifact caused by the
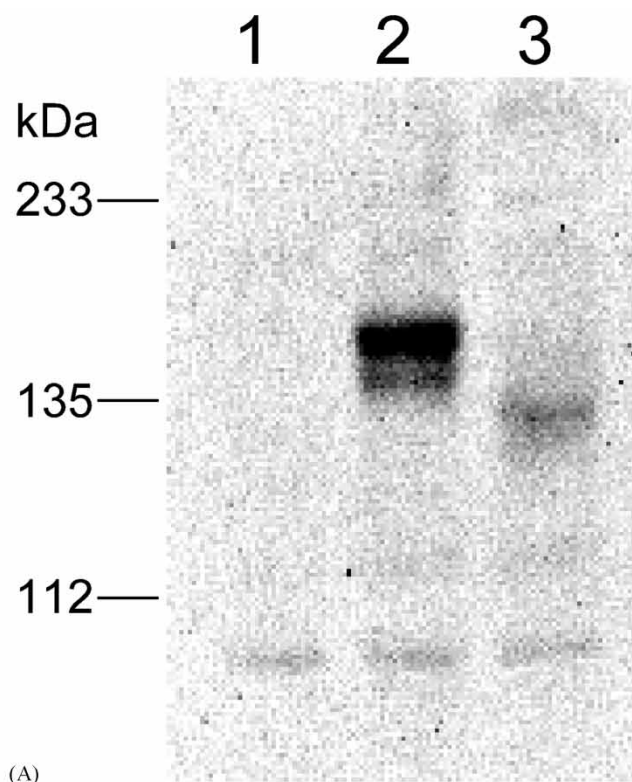
(A)
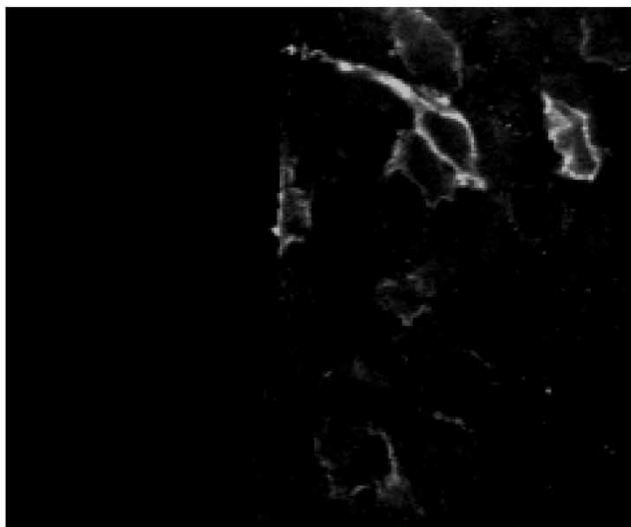
(B)
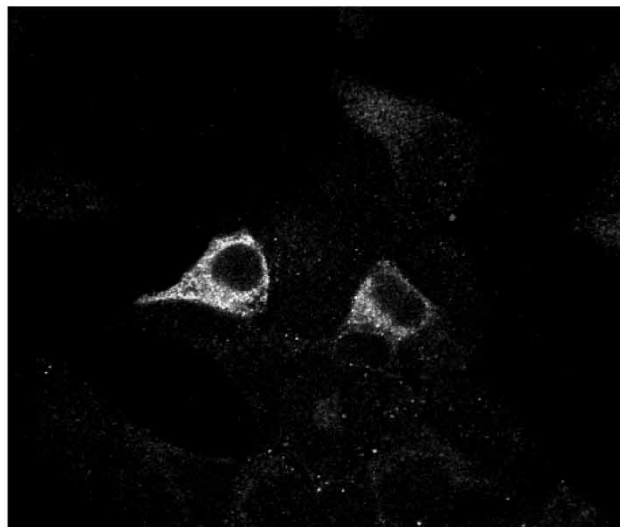
(C)

Figure 2.   Expression and localization of HANBC3 and HANBC3ΔCt. (*a*) HEK 293 cells transfected with empty vector (lane 1), HANBC3 (lane 2) or HANBC3ΔCt (lane 3) were solubilized and samples (5 µg protein) were resolved by SDS–PAGE and transferred to PVDF membrane. Immunoblot as probed with rabbit polyclonal anti-HA anti-body. Localization of HANBC3 (*b*) and HANBC3ΔCt (*c*) was assessed by confocal microscopy of transiently transfected HEK293. Coverslips were fixed, permeablized and stained with the same anti-HA anti-body as above, a biotinylated goat anti-rabbit secondary anti-body and, finally, streptavidin-FITC dye.

high concentration of the sample. Fractions from reverse phase HPLC peaks were analysed by mass spectrometry and the NBC3Ct peak was found to elute at $\sim$ 23 min. Integration of this peak indicated a sample purity of $\sim$ 97%, which is slightly greater than densitometry showed.

Hydrodynamic shape analysis of NBC3CT

The Stokes radius of NBC3Ct was 26 Å, on the basis of elution from GPC columns. This was surprising since this is greater than the Stokes radius of the carbonic anhydrase standard, which has more than twice the molecular weight of

Table 1. Summary of NBC3Ct purification data. Purification units were based on the desitometric analysis of the appropriate bands in Figure 3.

Step	Culture	Cleared lysate	Affinity resin	Cleaved fusion	Post GPC
units*	206	188	7	8	6
% yield	/	91	4	4	3
% purity	20	18	67	48	94
yield (mg)	/	151	/	/	4

* Units were assigned based on the number of pixels counted during densitometry of the scanned gel. Each count was normalized for the fraction of total protein used and divided by 10 000 000 pixels. Per cent yield was calculated from the units remaining compared to the resuspended culture. Per cent purity was determined by comparing the pixels representing the band of interest to the total pixels for a given lane.

NBC3Ct. The observation was verified independently by sedimentation velocity analysis, which indicated a Stokes radius of 30 Å and an axial ratio of 12:1. Shape modelling using the Teller method indicated a prolate molecule with long and short axial diameters of 19 and 2 nm, respectively (Figure 4(b)).

NBC3Ct conformation is insensitive to changes in pH and temperature

Purified NBC3Ct was analysed by CD spectroscopy over the pH range 6.2–7.8 (Figure 5(a)). Secondary structure of NBC3Ct was insensitive to changes of pH over the patho/ physiological range, as indicated by the nearly super-imposable CD spectra from 5 pH values assessed. Best fit de-convolution modelling, as analysed using the Contin programme of Provencher and Glockner (1981), indicated 60% β-sheet, 33% β-turn and 7% random coil at pH 7.0. The range of $\Delta\varepsilon$ seen was not very large, ~ -2500 M^{-1} cm^{-1} at 215 nm compared to a fully β-structured protein ($\sim -30\,000$ M^{-1} cm^{-1} at 215 nm), which suggests that, although the total structure is predominantly β, NBC3Ct likely does not form a single continuous β-sheet. Interestingly, thermal denaturation CD scans indicated a subtle loss of β-structure in the 5–25 °C range but the majority of structure was retained up to 85 °C, which suggests that NBC3Ct is very stable (not shown).

Identification of surface exposed regions of NBC3Ct

Limited proteolysis was used to identify regions of the domain that are sensitive to proteolysis, suggesting an extended or open structure. The amino acid sequence of NBC3Ct contains 19 and 17 potential trypsin and chymo-trypsin cleavage sites, respectively, distributed throughout the length of the domain (Figure 6(d)). Thus, digestion with these enzymes should identify open-structured parts of the whole domain. Tryptic digests were optimized to identify the concentration of trypsin producing a ladder of fragments following 20 min of digestion. Using this method 40 µg/ml trypsin was selected for longer time courses. Figure 6(a) shows the results of a 64 min digestion, which resulted in nearly complete cleavage of the starting material (Figure 6(a)). When the same optimization protocol was used to identify an appropriate chymotrypsin concentration, even at low concentrations of enzyme, all starting material had been digested by 20 min. A stable fragment appeared within the first 30 s of digestion (Figure 6(b)).

Samples of both reactions from each time point were analysed by matrix-assisted laser desorption/ionization-time of flight mass spectroscopy for fragments between 5–25 kDa (m/z). Resolution of the technique was ± 4 Da, which was sufficient to determine the sites of cleavage of NBC3Ct (Figure 6(c)). Also, the relative intensity of each fragment at each time point indicated the order of degradation and relative site sensitivity (Figure 6(c)). That is, more sensitive sites rise in intensity earlier than less sensitive sites. In order of cleavage, trypsin cleaved at sites R1129, K1186 and K1183. After 8 min the fragment cleaved at R1129 and K1183 (6341 Da) was stable and persisted through until the end of the experiment (64 min). Chymotrypsin cleaved only at one site (yielding a fragment greater than 5 kDa), at L1185.

Discussion

The C-terminal domains of bicarbonate transporter super-family members play an important role in the regulation of transport function (Pushkin *et al.* 2000a, Sterling *et al.* 2001a, Weinman *et al.* 2001). AE1, AE2, AE3 (Sterling *et al.* 2001a, Gross *et al.* 2002) and NBC1 (Gross *et al.* 2002, Alvarez, Loiselle and Casey, submitted for publication) bind the cytosolic enzyme, carbonic anhydrase II. Mutation of the CAII binding site or competitive displacement of CAII from its binding site diminished HCO_3^- transport activity by $\sim 40\%$ for these transporters. Recently it has been suggested that phosphorylation of the C-terminal domain of NBC1 may modulate the HCO_3^-/Na^+ coupling ratio by displacement of CAII from its binding site (Gross *et al.* 2002). This finding suggests that the bicarbonate transporter/CAII interaction may be regulated in a phosphorylation-state dependant manner. The C-terminal domain of NBC3 likely plays a similarly important role. The present report found that deletion of the C-terminal domain of NBC3 reduced transport by almost 90% (Figure 1), consistent with an important role for the domain. NBC3Ct has an open structure, well suited to act as a binding site for peripheral proteins, but the domain does not undergo conformational alterations with changes of cytosolic pH. If NBC3Ct mediates regulation of transport in response to changes of cytosolic pH, it does not do so by changes to its secondary structure.

Immunoblotting of transiently transfected HEK293 cells identified two specific bands for NBC3, migrating at ~ 168 and ~ 156 kDa. The higher molecular weight band is not as large as previously reported, but this likely reflects a tissue-type specific glycosylation pattern and not a difference in
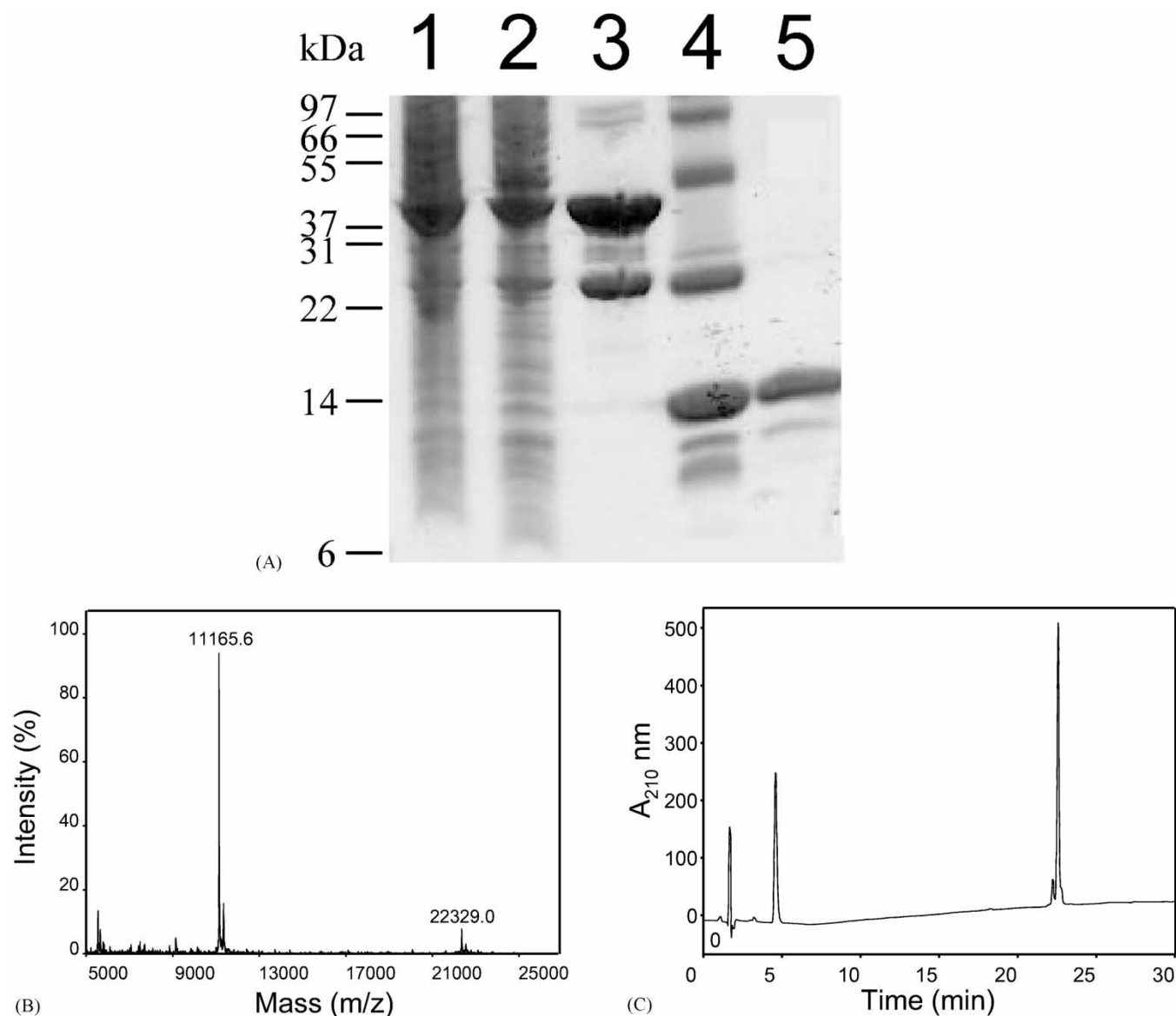
Figure 3. Analysis of NBC3Ct purification. (*a*) Samples from stages of the purification procedure were subjected to SDS−PAGE on 15% acrylamide gels and Coomassie blue staining. An equal fraction of total protein was loaded in each lane. Sample analyses were resuspended culture following 3 h of induction with 1 mM IPTG (lane 1), Triton X-100 treated lysate (lane 2), Glutathione Sepharose® 4B resin incubated with the lysate and washed extensively (lane 3), supernatant from PreScission™ protease treated resin (lane 4) and GPC chromatography purified sample (lane 5). (*b*) The purified sample was analysed by matrix-assisted laser desorption/ionisation-time of flight mass spectrometry, which indicated a nearly pure protein at the predicted molecular weight of 11 165 Da. (*c*) Reverse phase high performance liquid chromatography analysis of the purified sample. Fractions were analysed by mass spectroscopy, the NBC3Ct peak was found to elute at ∼23 min and showed 97% purity.

primary sequence. The deletion mutant migrated at ∼10 kDa less than the lower NBC3 band, as expected based on the predicted molecular weight of the C-terminal domain. The lack of a corresponding higher molecular weight band for the C-terminal deletion mutant suggests that the deletion is either un- or incompletely glycosylated. This suggests that the lower NBC3 band and the deletion mutant band are equally glycosylated or unglycosylated. Thus, it is likely that the poor transport activity of the C-terminal deletion mutant is secondary to poor processing to the plasma membrane. Consistent with this idea, confocal microscopy of HEK293

cells transiently transfected with either NBC3 or the deletion mutant showed greater sub-cellular retention of the deletion mutant (Figure 2(*b*) and (*c*)).

The fusion protein, GST.NBC3Ct, which was over-expressed to 20% of total protein (Figure 3(*a*)), was almost completely soluble as assessed by densitometry. The very high purity of NBC3Ct gave confidence that the biochemical characterizations were accurate and not influenced to any significant extent by impurities. During purification, it was found that NBC3Ct eluted from the GPC column much earlier than was expected based on its molecular weight. The
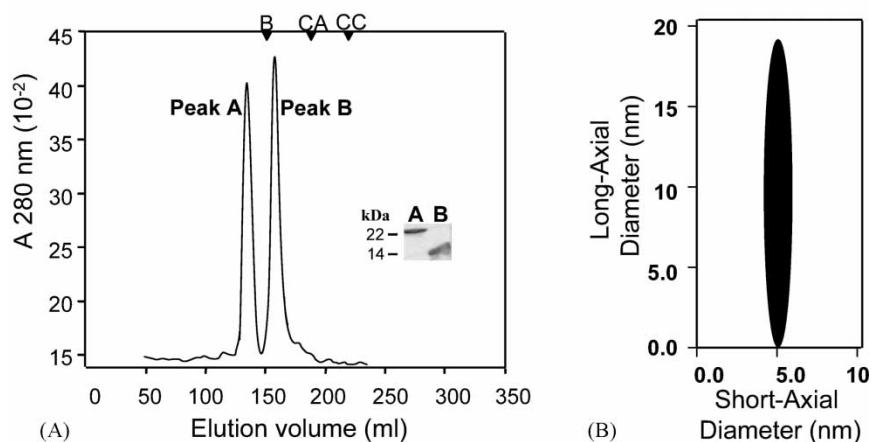
Figure 4. Shape analysis of NBC3Ct. (*a*) PreScission™ protease treated GST.NBC3Ct was applied to a Superdex® 75 column via a Pharmacia Biotech FPLC apparatus and 5 ml fractions were collected. The fractions corresponding to peaks A and B were pooled separately and analysed by SDS-PAGE with Coomassie blue staining (inset) and immunoblotting (not shown). Arrows indicate the elution position of bovine serum albumin (B, 36 Å, 66 kDa), carbonic anhydrase (CA, 20 Å, 29 kDa), cytochrome C (CC, 16 Å, 12.4 kDa). The Stokes radius for peak B was found to be 26 Å. (*b*) Shape modelling by Sedimentation Velocity. Purified NBC3Ct was subjected to analytical ultracentrifugation in a Beckman XL-I ultracentrifuge. Data was analysed using the programme, SEDNTERP. Analysis indicated a Stokes radius of 29.6 Å and an axial ratio of 12.2. The model was generated by SEDNTERP on the basis of these parameters and the amino acid sequence of the domain; it indicates a prolate shape with a long axis of 19 nm and a short axis of 1.6 nm.
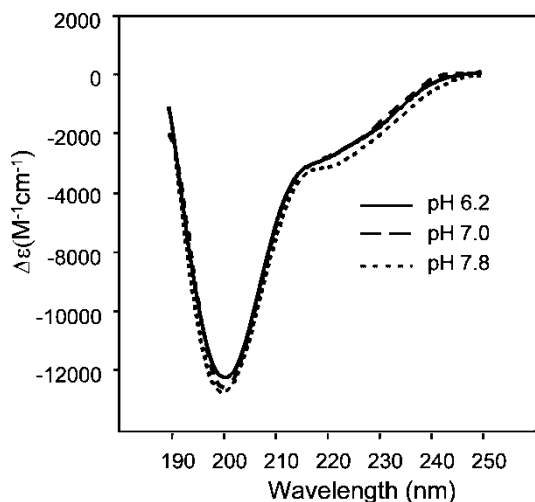

Figure 5. Circular dichroism spectroscopy of NBC3Ct at a range of pH values. Circular dichroism spectra were collected in Phosphate buffers at pH 6.2, 7., and 7.8. Each curve was generated from the average of eight scans of the same sample.

Stokes radius of 26 Å was independently verified by velocity ultracentrifugation, which indicated a Stokes radius of 30 Å. Using modelling software, a rod-like shape ~ 19 nm long by ~ 2 nm wide was predicted. NBC3Ct possesses a PDZ consensus binding motif that shares strong homology to the PDZ motif of Na$^+$/H$^+$-exchanger 3, which has been shown to interact with cytoskeletal scaffolding elements and A kinase anchor proteins (Kim *et al.* 2002). An extended structure would be ideal to bind such regulatory proteins and to form sites for anchorage to the cytoskeleton.

NBC1 activity was sensitive to changes in intracellular pH but not extracellular pH (Gross and Hopfer 1999). It, thus, seems likely that pH sensitivity is conferred by one or more of the cytoplasmic domains or/and intracellular loop of the membrane domain. It was hypothesized that the C-terminal domain could undergo a pH-dependent conformational change within the physiological or pathophysiological range. Measuring secondary structure as an indication of conformation, one could not detect any change within the pH range examined. This finding suggests either (a) that the C-terminal domain does not contain a pH sensor or (b) a C-terminal pH sensor does not function via substantial secondary structure changes. It was concluded that, within the sensitivity limits of circular dichroism spectroscopy, NBC3Ct does not undergo pH-dependent changes of secondary structure. However, one cannot rule out the possibility that reorientation of structural elements occurs as a function of pH. That is, the domain could open and close in a hinge-like manner, without change of secondary structure, but with a large change in conformation. Such pH-dependent changes of structure are found in the N-terminal cytoplasmic domain of the Cl$^-$/HCO$_3^-$ exchanger, AE1 (Zhang *et al.* 2000).

NBC3Ct has a large number of trypsin and chymotrypsin sites distributed throughout the length of the polypeptide, which makes it particularly amenable to study by limited proteolysis. Digestion experiments were designed to identify the first few cleavage sites utilized because these are most likely to be the most accessible surface exposed residues. Since trypsin and chymotrypsin cleave at basic and hydrophobic residues, respectively, it was expected that trypsin would generate more fragments than chymotrypsin. Hydro-pH$_i$lic residues are more prevalent at the surface of proteins, while hydrophobic residues generally make up the core of proteins. Indeed, trypsin and chymotrypsin cleavage generated three and one fragments, respectively, under similar conditions. Given that NBC3Ct has such a long shape, it was surprising that proteolysis generated so few cleavages under the experimental conditions, especially for trypsin. NBC3Ct also contains several acidic residues, leading to an isoelectric pH of 6.20, with 22% basic residues and 25% acidic

Trypsinolysis

Time (min)	0	2	4	8	16	32	64

(A)

Chymotrypsinolysis

Time (min)	0	0.5	1	2	4	8	16

(B)

(C)
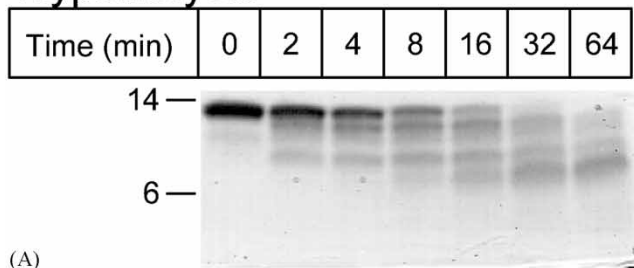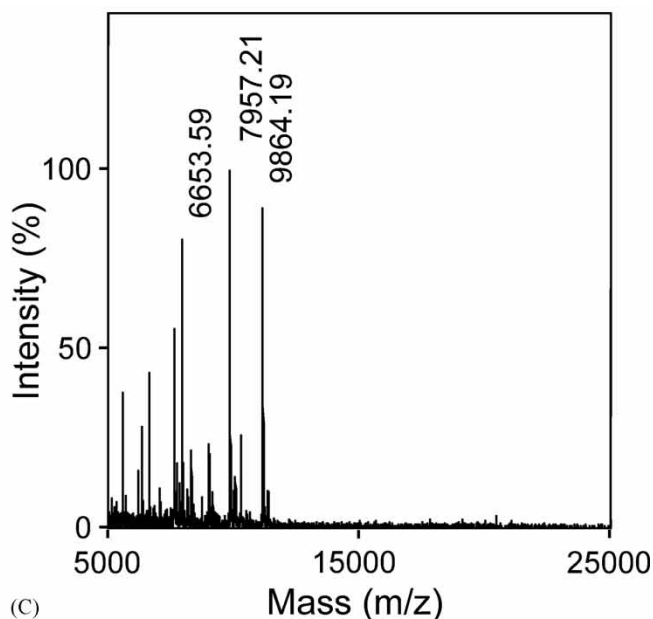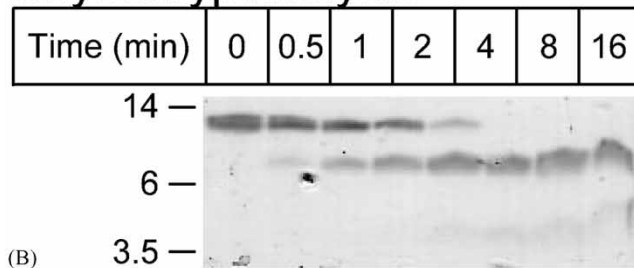
NH₂-GPLGSPEFMTK̲R̲ELSW̲L̲DDL̲MPESK̲K̲K̲K̲EDDK̲K̲K̲K̲EKEEA̲ERM̲L̲QDDDDT

VHL̲PE̲EGGSL̲L̲QIPVK̲AL̲K̲YSPDK̲PVSVK̲ISE̲EDEPR̲K̲K̲YVDAETSL̲-COOH

(D)

Figure 6. Limited proteolysis of NBC3Ct using trypsin and chymotrypsin. Coomassie Blue stained SDS−PAGE gels of the progression of trypsinolysis (*a*) and chymotrypsinolysis (*b*), respectively, of NBC3Ct. Three and one distinct proteolytic fragments are observed during trypsinolysis and chymotrypsinolysis, respectively. (*c*) The molecular weight of each fragment was determined by matrix-assisted laser desorption/ionisation-time of flight mass spectrometry; a sample output for the 4 min time point (trypsinolysis) is shown. (*d*) Model of the sequence of NBC3Ct with the observed cleavage sites indicated by * above the sequence. Potential cleavage sites are indicated under the sequence by − and = for trypsin and chymotrypsin, respectively.

residues. One explanation for the low number of sites used may be that the majority of charged residues are ion paired or otherwise made immobile via solvent interactions and, therefore, less susceptible to cleavage.

Sites identified as protease-sensitive are, by definition, accessible to interacting proteins and are, therefore, candidates for sites of interaction with peripheral proteins. Although these sites represent the best candidates for peripheral binding, it does not rule out the possibility that other parts of NBC3Ct could interact with other proteins. Proteolytic cleavage sites clustered around two regions. One was at the N-terminal end of NBC3Ct just after the membrane domain (Figure 6(*d*)). The accessibility the N-terminal region suggests that the purified domain has assumed a native conformation, since this region is required to be at the surface of the C-terminal domain because of its attachment to the membrane domain. Interestingly, sequence analysis indicates that a consensus PKA phosphorylation site, S1132, is three residues C-terminal to the cleavage site and a consensus CAII binding site lies five residues C-terminal to the cleavage site. Taken together, this data suggests a model in which a CAII binding site and a PKA phosphorylation site localize to an open region on the

extended rod structure of the NBC3 C-terminal tail. A similar region was recently identified in NBC1. Mutation of D986 or D988 blocked the S982 phosphorylation-state dependent shift from 2:1 to 3:1, HCO_3^-:Na^+ transport stoichiometry for NBC1 (Gross *et al.* 2002). It seems likely that this region also undergoes a phosphorylation-state-dependent interaction with CAII. One is currently investigating this possibility.

The second proteolytic sensitive region spans K1183 to K1186. Chymotrypsin also cleaved at L1185, between the two lysine residues. Chymotrypsin cleaves aromatic residues at a higher rate than leucine, which suggests that the accessible motif is limited at its C-terminal end by K1186 since no detectable cleavage occurred at Y1187. NBC3 shows cell type specific membrane targeting, apical or basolateral in type A and B intercalated cells, respectively (Pushkin *et al.* 1999b, Kwon *et al.* 2000). Assuming that the N-terminal accessible binding region is involved in regulation of transport activity through binding to CAII, region 2 may be involved in cell surface targeting.

In conclusion, NBC3Ct is required for membrane targeting and mediation of CAII binding. Consistent with NBC3 in the kidney, it was also found that NBC3 localizes both to the plasma membrane and to an intracellular pool. Structural

analysis revealed NBC3Ct as a stable elongated rod-like shape with two proteolytically sensitive regions. This structure is well-suited to a role in binding of regulatory proteins. NBC3Ct did not change structure over the pH range tested, suggesting that secondary structure changes do not serve to signal changes of NBC3 activity. NBC3Ct proximal to the membrane domain contains consensus CAII binding and PKA phosphorylation motifs and had an open, accessible structure. Thus, the region could be involved in mediation of a phosphorylation state dependent interaction with CAII. The membrane-distal region of NBC3Ct may be involved in membrane targeting.

Experimental procedures

Materials

Human NBC3 cDNA was a generous gift from Ira Kurtz (U.C.L.A.). PCR primers were from Life Technologies Inc. Recombinant expression vector, pGEX-6p-1, and ECL reagent were from Pharmacia Biotech. Pwo DNA polymerase was from Roche and all other cloning enzymes were from New England Biolabs. *Escherichia coli* recombinant expression strain, BL21-CodonPlus was from Stratagene. Protein concentrators were from Millipore. GST fusion purification reagents, FPLC apparatus and HiLoad 26/60 Superdex 75 gel permeation columns were from Pharmacia Biotech. Amino-acid analysis was provided by Alberta Peptide Institute, Edmonton, Canada. Transfection and cell culture reagents were from Invitrogen.

DNA constructs

NBC3 C-terminal domain (NBC3Ct) corresponding to codons 1127−1214 of NBC3 cDNA was amplified by PCR using the forward and reverse primers 5′-GGAATTGAATTCATGACGAAGAGAGAACT-TAGTTGGCTTGA and 3′-CCTTAAGGGCGGCCGCTACTATAAT-GAAGTTTCAGCATCCACGTA, respectively. pGEX-6p-1 and the PCR product were digested with BamH I and Not I and ligated, yielding pNBC3Ct.

The carboxyl terminal deletion construct (NBC3ΔCt) coded for the entire NBC3 cDNA except nucleotides 2865−3378. A stop codon and a Not I site were introduced at the 3′ end of the product. The forward and reverse primers used were 5′-GCTCATGGTTGGCGT-TATGTTGG and 3′-CCTTAACCGAATTCCTACTAGAAACACAGG-TCCATGAGTTTGCGC, respectively. The PCR product and the NBC3 expression construct were digested with Eco R I and Not I, the fragments were ligated, yielding pNBC3ΔCt.

An HA epitope tag was added to the end of the N-terminus of both NBC3 and NBC3ΔCt. An Nhe I restriction site, new start codon and the HA epitope were built into the forward PCR primer, 5′-GGAACGAGCTAGCATGTACCCCTACGACGTGCCCGACTACGC-C ATGGAAAGA TTTCGTCTGG AGAAG and reverse primer was CCACATAAGGTTTACTCC. The PCR product was amplified using human NBC3 cDNA as a template. NBC3 and NBC3ΔCt were digested with Nhe I and BstE II and were ligated, yielding pHANBC3 and pHANBC3ΔCt, respectively.

Protein expression in mammalian cells

NBC3 protein was expressed by transient transfection of HEK293 cells (Choi *et al.* 1999, Sterling *et al.* 2001b) using the calcium phosphate method (Ruetz *et al.* 1993). All experiments with transfected cells were carried out 48-h post-transfection. Cells were grown at 37 °C in an air/CO$_2$ (19:1) environment in Dulbecco's modified Eagle media (DMEM), supplemented with 5% (v/v) foetal bovine serum and 5% (v/v) calf serum.

NBC3 transport assay

The transport activity of NBC3 was monitored using a fluorescence assay, as previously described (Khandoudi *et al.* 2001). Briefly, HEK293 cells grown on poly-L-lysine coated coverslips were transiently transfected, as described in the previous section. Forty-eight hours post-transfection, coverslips were rinsed in serum free DMEM and incubated in 4 ml serum-free media, containing 2 μM 2′,7′-bis-(2-carboxyethyl)-5-(and-6)-carboxyfluorescein-acetoxy-methyl ester (37 °C, 20 min). Coverslips were mounted in a fluorescence cuvette and perfused with Ringers buffer (5 mM glucose, 5 mM K gluconate, 1 mM Ca gluconate, 1 mM MgSO$_4$, 10 mM Hepes, 140 mM NaCl, 2.5 mM NaH$_2$PO$_4$, 25 mM NaHCO$_3$, pH 7.4), equilibrated with 5% CO$_2$/air. pH$_i$ recovery activity was measured during the recovery from transient intracellular acidification. Acid loading was accomplished by transient perfusion with Ringers buffer, containing 40 mM NH$_4$Cl for 5 min, followed by the wash-out of NH$_4$Cl with Ringers buffer. All experiments were performed in the presence of 10 μM 5-(N-ethyl-N-isopropyl) amiloride (Sigma) to block endogenous NHE activity. Fluorescence was monitored using a Photon Technologies International RCR fluori-meter, at excitation wavelengths 440 and 500 nm and emission wavelength 530 nm. Following calibration using the nigericin/high potassium technique (Thomas *et al.* 1979) at three pH values between 6.5−7.5, fluorescence ratios were converted to pH$_i$. The initial rate of pH$_i$ recovery from an acid load was calculated by linear regression of the first 1 min or the first 3 min of the pH$_i$ recovery after maximum acidosis. The rates of HCO$_3^-$ influx (J_{HCO} in mM/min) were estimated according to the equation $J_{HCO} = \beta_{total} \times \Delta pH_i$ (Roos and Boron 1981), where $\beta_{total} = \beta_i + \beta_{CO_2}$, $\beta_i = 10$ mM (Sterling and Casey 1999) and $\beta_{CO_2} = 2.3 \times [HCO_3^-]$. In all cases the transport activity of cells transfected with empty vector was subtracted from the total rate, to ensure that these rates consisted only of HANBC3 or HANBC3ΔCt transport activity.

Immunodection

Transfected cells were washed in PBS buffer (140 mM NaCl, 3 mM KCl, 6.5 mM Na$_2$HPO$_4$, 1.5 mM KH$_2$PO$_4$, pH 7.5) and lysates of the whole tissue culture cells were prepared by addition of 150 μl SDS−PAGE sample buffer (20% (v/v) glycerol, 2% (v/v) 2-mercaptoethanol, 4% (w/v) SDS, 1% (w/v) Bromophenol Blue, 150 mM Tris, pH 6.8) containing complete mini protease inhibitor cocktail (Roche). Prior to analysis, samples were heated to 65 °C for 5 min and sheared through a 26-gauge needle (Becton Dickinson). Insoluble material was then sedimented by centrifugation at 16 000 × g for 10 min. Total protein content was measured using the Bradford protein assay (Bradford 1976). Samples (5 μg) were resolved by SDS−PAGE on 8% acrylamide gels (Laemmli 1970). Proteins were transferred to PVDF membranes by electrophoresis for 2 h at 100 V at room temperature, in buffer composed of 20% (v/v) methanol, 25 mM Tris and 192 mM glycine (Towbin *et al.* 1979). PVDF membranes were blocked by incubation for 1 h in TBST-M buffer (TBST buffer (0.1% (v/v) Tween-20, 137 mM NaCl, 20 mM Tris, pH 7.5), containing 5% (w/v) non-fat dry milk) and then incubated overnight in 10 ml TBST-M, containing 20 μl rabbit anti-HA anti-body. The next day, blots were washed thee times with TBST and then incubated with TBSTM containing 1:3000 diluted donkey anti-rabbit IgG conjugated to horseradish peroxidase. After a final wash with TBST buffer (three times), blots were visualized using ECL reagent and a Kodak Image Station 440CF.

Confocal microscopy

Cells grown on poly-L-lysine-coated, 18 mm diameter coverslips were transiently transfected as described. The coverslips were transferred to 35 mm Petri dishes. Cells were fixed for 30 min in 2% (w/v) paraformaldehyde in PBSC (PBS, containing 1 mM CaCl$_2$). After two washes with PBSC, the cells were incubated for 25 min in permeabilization buffer (300 mM sucrose, 50 mM NaCl, 3 mM MgCl$_2$, 0.5% (v/v) Triton X-100, 20 mM Hepes, pH 7.4). Coverslips were washed three times with PBSC and blocked for 25 min in 10% serum in PBSC. Coverslips were incubated with 1/50 dilution of rabbit anti-

HA anti-body SC805 in PBSCS (PBSC, containing 4% serum). Coverslips were washed three times with PBSCS, and incubated for 45 min in the dark with 1/100 dilution of biotinylated anti-rabbit IgG anti-body in PBSCS. After three washes with PBSCS, coverslips were incubated for 45 min in the dark with 1/100 dilution of streptavidin fluorescein conjugate. Images were collected using a Zeiss LSM 510 laser scanning confocal microscope mounted on an Axiovert 100M, with a $63 \times$ (NA1.4) lens.

GST-fusion protein purification

GST.NBC3Ct was expressed in pGST.NBC3Ct-transfomed *E. coli* BL21 codon plus. Protein from 1.2 l culture was purified by glutathione Sepharose affinity chromatography, as previously described. The fusion protein on glutathione Sepharose was washed three times with PreScission cleavage buffer (150 mM NaCl, 1 mM EDTA, 1 mM dithiothreitol, 50 mM Tris−HCl, pH 7.0). PreScission Protease (60 units/ml resin) was then added and the sample incubated at 4 °C for 48 h with rotation. Following cleavage, the resin was centrifuged $500 \times g$ for 5 min and the supernatant collected. Resin was washed with an equal volume of cleavage buffer and the supernatants pooled. Cleaved fusion protein was then further purified by FPLC gel permeation chromatography using a HiLoad 26/60 Superdex 75 column, eluted with GPC buffer (150 mM NaCl, 1 mM DTT, 50 mM Tris−HCl, pH 7.5). Fractions (5 ml) were collected. Peak fractions were pooled and designated Peak A and Peak B.

Analytical ultracentrifugation

Sedimentation velocity experiments were conducted at 5 °C in a Beckman XL-I analytical ultracentrifuge using absorbance optics (Laue and Stafford 1999). Aliquots (400 μl) of sample were loaded into 2-sector CFE sample cells and centrifuged at 60 000 rpm for ~ 3 h, during which a minimum of 50 scans were collected. Sedimentation coefficients were determined with the program SVEDBERG (Philo 1997), which incorporates a modified Fujita-MacCosham function into a non-linear least squares fitting routine to fit the sedimentation boundaries to either single species or multiple species models. The program SEDNTERP was employed to calculate the protein's partial specific volume, $S_{20,w}$, axial ratio and the solvent density and viscosity (Laue and Stafford 1999).

Circular dichroism spectroscopy

pH titration experiments were performed using a JASCO J-720 spectropolarimeter. NBC3Ct at 7.1 mM in CD buffer (15 mM Hepes, 100 mM KCl) was scanned at pH values 6.2, 6.8, 7.0, 7.2 and 7.8 at 25 °C. Experiments were performed with the following conditions: cell length 0.2 mm, scan range 196−250 nm, resolution 1 nm, sensitivity 50 mdeg, response 0.25 s, speed 50 nm/min, and eight accumulations per sample. In thermal denaturation experiments, 2.2 mM NBC3Ct in TDCD buffer (25 mM NaPO₄, 50 mM NaCl, pH 7.5) were scanned at 5, 15, 25, 35, 45, 55, 65 and 75 °C. Experiments were performed under the following conditions: cell length 1 mm, scan range 203−250 nm, resolution 1 nm, sensitivity 20 mdeg, response 0.25 s, speed 100 nm/min and eight accumulations per sample. All data were analysed using JASCO J700 analysis software.

Proteolysis

NBC3Ct in GPC buffer was digested with 1 μg/ml chymotrypsin and 40 μg/ml trypsin at 25 °C. Reactions were quenched by the addition of two SDS−PAGE sample buffer and immediately boiling samples for 5 min. Alternatively, samples for mass spectroscopy analysis were quenched by transferring aliquots to glacial acetic acid (25% final concentration). Mass spectroscopy samples were analysed by matrix-assisted laser desorption/ionisation-time of flight (Voyager De-Pro from ABI) and dominant fragment weights were screened against a library of predicted fragment weights and fragment

designations assigned. Samples (20 μg) were also loaded onto 15% SDS-PAGE gels, electrophoresed and stained with Coomassie Blue.

References

Abuladze, N., Lee, I., Newman, D., Hwang, J., Boorer, K., Pushkin, A. and Kurtz, I., 1998, Molecular cloning, chromosomal localization, tissue distribution, and functional expression of the human pancreatic sodium bicarbonate cotransporter. *Journal of Biological Chemistry*, **273**, 17689−17695.

Alper, S. L., Chernova, M. N. and Stewart, A. K., 2001, Regulation of Na⁺-independent Cl⁻/HCO₃⁻ exchangers by pH. *Journal of Pancreas*, **2**, 171−175.

Amlal, H., Burnham, C. E. and Soleimani, M., 1999, Characterization of Na⁺/HCO₃⁻ cotransporter isoform NBC-3 [published erratum appears in American Journal of Physiology, 1999; 277: following table of contents]. *American Journal of Physiology*, **276**, F903−F913.

Avkiran, M. and Haworth, R. S., 1999, Regulation of cardiac sarcolemmal Na⁺/H⁺ exchanger activity by endogenous ligands. Relevance to ischemia. *Annals of the New York Academy of Science*, **874**, 335−345.

Bevensee, M. O., Schmitt, B. M., Choi, I., Romero, M. F. and Boron, W. F., 2000, An electrogenic Na⁺−HCO₃⁻ cotransporter (NBC) with a novel COOH-terminus, cloned from rat brain. *American Journal of Physiology*, **278**, C1200−C1211.

Boron, V. F., Hediger, M. A., Boulpaep, E. L. and Romero, M. F., 1997, The renal electrogenic Na⁺:HCO₃⁻ cotransporter. *Journal of Experimental Biology*, **200**, 263−268.

Bradford, M. M., 1976, A rapid and sensitive method for the quantitation of microgram quantities of protein utilizing the pricinple of protein-dye binding. *Analytical Biochemistry*, **72**, 248−254.

Burnham, C. E., Flagella, M., Wang, Z., Amlal, H., Shull, G. E. and Soleimani, M., 1998, Cloning, renal distribution, and regulation of the rat Na⁺−HCO₃⁻ cotransporter. *American Journal of Physiology*, **274**, F1119−F1126.

Choi, I., Romero, M. F., Khandoudi, N., Bril, A. and Boron, W. F., 1999, Cloning and characterization of a human electrogenic Na⁺−HCO₃⁻ cotransporter isoform (hhNBC). *American Journal of Physiology*, **276**, C576−C584.

Choi, I., Aalkjaer, C., Boulpaep, E. L. and Boron, W. F., 2000, An electroneutral sodium/bicarbonate cotransporter NBCn1 and associated sodium channel. *Nature*, **405**, 571−575.

Chow, C. W., 1999, Regulation and intracellular localization of the epithelial isoforms of the Na⁺/H⁺ exchangers NHE2 and NHE3. *Clinical Investigations in Medicine*, **22**, 195−206.

Gross, E. and Hopfer, U., 1999, Effects of pH on kinetic parameters of the Na⁺/HCO₃⁻ cotransporter in renal proximal tubule. *Biophysics Journal*, **76**, 3066−3075.

Gross, E., Abuladze, N., Pushkin, A., Kurtz, I. and Cotton, C. U., 2001, The stoichiometry of the electrogenic sodium bicarbonate cotransporter pNBC1 in mouse pancreatic duct cells is 2 HCO₃⁻:1 Na⁺. *Journal of Physiology*, **531**, 375−382.

Gross, E., Pushkin, A., Abuladze, N., Fedotoff, O. and Kurtz, I., 2002, Regulation of the sodium bicarbonate cotransporter kNBC1 function: role of Asp(986), Asp(988) and kNBC1-carbonic anhydrase II binding. *Journal of Physiology*, **544**, 679−685.

Hara, C., Satoh, H., Usui, T., Kunimi, M., Noiri, E., Tsukamoto, K., Taniguchi, S., Uwatoko, S., Goto, A., Racusen, L. C., Inatomi, J.,

Endou, H., Fujita, T. and Seki, G., 2003, Intracellular pH regulatory mechanism in a human renal proximal cell line (HKC-8): evidence for Na^+/H^+ exchanger, Cl^-/HCO_3^- exchanger and Na^+/HCO_3^- cotransporter. *Pflugers Archives*, **440**, 713–720.

Hume, J. R., Duan, D., Collier, M. L., Yamazaki, J. and Horowitz, B., 2000, Anion transport in heart. *Physiology Reviews*, **80**, 31–81.

Igarashi, P., Reilly, R. F., Hildebrandt, F., Biemesderfer, D., Reboucas, N. A., Slayman, C. W. and Aronson, P. S., 1991, Molecular biology of renal Na^+/H^+ exchangers. *Kidney International Supplement*, **33**, S84–S89.

Juel, C., 1996, Lactate/proton co-transport in skeletal muscle: regulation and importance for pH homeostasis. *Acta Physiologica Scandinavia*, **156**, 369–374.

Khandoudi, N., Albadine, J., Robert, P., Krief, S., Berrebi-Bertrand, I., Martin, X., Bevensee, M. O., Boron, W. F. and Bril, A., 2001, Inhibition of the cardiac electrogenic sodium bicarbonate cotransporter reduces ischemic injury. *Cardiovascular Research*, **52**, 387–396.

Kim, J. H., Lee-Kwon, W., Park, J. B., Ryu, S. H., Yun, C. H. and Donowitz, M., 2002, Ca^{2+}-dependent inhibition of Na^+/H^+ exchanger 3 (NHE3) requires an NHE3-E3KARP-alpha-actinin-4 complex for oligomerization and endocytosis. *Journal of Biological Chemistry*, **277**, 23714–23724.

Komukai, K., Ishikawa, T. and Kurihara, S., 1998, Effects of acidosis on Ca^{2+} sensitivity of contractile elements in intact ferret myocardium. *American Journal of Physiology*, **274**, H147–H54.

Kwon, T. H., Pushkin, A., Abuladze, N., Nielsen, S. and Kurtz, I., 2000, Immunoelectron microscopic localization of NBC3 sodium-bicarbonate cotransporter in rat kidney. *American Journal of Physiology Renal Physiology*, **278**, F327–F336.

Laemmli, U. K., 1970, Cleavage of structural proteins during assembly of the head of bacteriophage T4. *Nature*, **227**, 680–685.

Laue, T. M. and Stafford 3rd, W. F., 1999, Modern applications of analytical ultracentrifugation. *Annual Review of Biophysics and Biomolecular Structures*, **28**, 75–100.

Leviel, F., Eladari, D., Blanchard, A., Poumarat, J. S., Paillard, M. and Podevin, R. A., 1999, Pathways for HCO_3^- exit across the basolateral membrane in rat thick limbs. *American Journal of Physiology*, **276**, F847–F856.

Lieberman, D. M. and Reithmeier, R. A. F., 1988, Localization of the carboxyl terminus of Band 3 to the cytoplasmic side of the erythrocyte membrane using antibodies raised against a synthetic peptide. *Journal of Biological Chemistry*, **263**, 10022–10028.

Lubman, R. L. and Crandall, E. D., 1992, Regulation of intracellular pH in alveolar epithelial cells. *American Journal of Physiology*, **262**, L1–L14.

Park, M., Ko, S. B., Choi, J. Y., Muallem, G., Thomas, P. J., Pushkin, A., Lee, M. S., Kim, J. Y., Lee, M. G., Muallem, S. and Kurtz, I., 2002, The cystic fibrosis transmembrane conductance regulator interacts with and regulates the activity of the HCO_3^- salvage transporter human $Na^+–HCO_3^-$ cotransport isoform 3. *Journal of Biological Chemistry*, **277**, 50503–50509.

Philo, J. S., 1997, An improved function for fitting sedimentation velocity data for low-molecular-weight solutes. *Biophysics Journal*, **72**, 435–444.

Provencher, S. W. and Glockner, J., 1981, Estimation of globular protein secondary structure from circular dichroism. *Biochemistry*, **20**, 33–37.

Pushkin, A., Abuladze, N., Lee, I., Newman, D., Hwang, J. and Kurtz, I., 1999, Cloning, tissue distribution, genomic organization, and functional characterization of NBC3, a new member of the sodium bicarbonate cotransporter family. *Journal of Biological Chemistry*, **274**, 16569–16575.

Pushkin, A., Yip, K. P., Clark, I., Abuladze, N., Kwon, T. H., Tsuruoka, S., Schwartz, G. J., Nielsen, S. and Kurtz, I., 1999, NBC3 expression in rabbit collecting duct: colocalization with vacuolar $H^+–ATPase$. *American Journal of Physiology*, **277**, F974–F981.

Pushkin, A., Abuladze, N., Newman, D., Lee, I., Xu, G. and Kurtz, I., 2000, Two C-terminal variants of NBC4, a new member of the sodium bicarbonate cotransporter family: cloning, characterization, and localization. *IUBMB Life*, **50**, 13–19.

Pushkin, A., Abuladze, N., Newman, D., Lee, I., Xu, G. and Kurtz, I., 2000, Cloning, characterization and chromosomal assignment of NBC4, a new member of the sodium bicarbonate cotransporter family. *Biochimica et Biophysica Acta*, **1493**, 215–218.

Romero, M. F., Hediger, M. A., Boulpaep, E. L. and Boron, W. F., 1997, Expression cloning and characterization of a renal electrogenic Na^+/HCO_3^- cotransporter. *Nature*, **387**, 409–413.

Romero, M. F., Fong, P., Berger, U. V., Hediger, M. A. and Boron, W. F., 1998, Cloning and functional expression of rNBC, an electrogenic $Na^+–HCO_3^-$ cotransporter from rat kidney. *American Journal of Physiology*, **274**, F425–F432.

Roos, A. and Boron, W. F., 1981, Intracellular pH. *Physiology Review*, **61**, 296–434.

Ruetz, S., Lindsey, A. E. and Kopito, R. R., 1993, Function and biosynthesis of erythroid and nonerythroid anion exchangers. *Society of General Physiologists Series*, **48**, 193–200.

Sassani, P., Pushkin, A., Gross, E., Gomer, A., Abuladze, N., Dukkipati, R., Carpenito, G. and Kurtz, I., 2002, Functional characterization of NBC4: a new electrogenic sodium-bicarbonate cotransporter. *American Journal of Physiology and Cell Physiology*, **282**, C408–416.

Sherman, M. and Goldberg, A. L., 1992, Involvement of the chaperonin dnaK in the rapid degradation of a mutant protein in Escherichia coli. *Embo Journal*, **11**, 71–77.

Sterling, D. and Casey, J. R., 1999, Transport activity of AE3 chloride/bicarbonate anion-exchange proteins and their regulation by intracellular pH. *Biochemistry Journal*, **344**, 221–229.

Sterling, D. and Casey, J. R., 2002, Bicarbonate transport proteins. *Biochemistry and Cell Biology*, **80**, 483–497.

Sterling, D., Reithmeier, R. A. and Casey, J. R., 2001, Carbonic anhydrase: in the driver's seat for bicarbonate transport. *Journal of Pancreas*, **2**, 165–170.

Sterling, D., Reithmeier, R. A. and Casey, J. R., 2001, A transport metabolon: Functional interaction of carbonic anhydrase II and chloride/bicarbonate exchangers. *Journal of Biological Chemistry*, **17**, 17.

Thevenod, F., Roussa, E., Schmitt, B. M. and Romero, M. F., 1999, Cloning and immunolocalization of a rat pancreatic Na^+ bicarbonate cotransporter. *Biochemical and Biophysics Research Communications*, **264**, 291–298.

Thomas, J. A., Buchsbaum, R. N., Zimniak, A. and Racker, E., 1979, Intracellular pH measurements in Ehrlich ascites tumor cells utilizing spectroscopic probes generated in situ. *Biochemistry*, **18**, 2210–2218.

Towbin, H., Staehelin, T. and Gordon, J., 1979, Electrophoretic transfer of proteins from polyacrylamide gels to nitrocellulose sheets: procedure and some applications. *Proceeding of the National Academy of Sciences (USA)*, **76**, 4350–4354.

Turner, H. C., Alvarez, L. J. and Candia, O. A., 2001, Identification and localization of acid–base transporters in the conjunctival epithelium. *Experimental Eye Research*, **72**, 519–531.

Wang, Z., Conforti, L., Petrovic, S., Amlal, H., Burnham, C. E. and Soleimani, M., 2001, Mouse $Na^+:HCO_3^-$ cotransporter isoform NBC-3 (kNBC-3): cloning, expression, and renal distribution. *Kidney International*, **59**, 1405–1414.

Weinman, E. J., Evangelista, C. M., Steplock, D., Liu, M. Z., Shenolikar, S. and Bernardo, A., 2001, Essential role for NHERF in cAMP-mediated inhibition of the Na^+/HCO_3^- co-transporter in BSC-1 cells. *Journal of Biological Chemistry*, **276**, 42339–42346.

Zhang, D., Kiyatkin, A., Bolin, J. T. and Low, P. S., 2000, Crystallographic structure and functional interpretation of the cytoplasmic domain of erythrocyte membrane band 3. *Blood*, **96**, 2925–2933.

Zhu, Q., Lee, D. W. K. and Casey, J. R., 2003, Novel topology in C-terminal region of the human plasma membrane anion exchanger, AE1. *Journal of Biological Chemistry*, **278**, 112–120.